The integral membrane protein ITM2A, a transcriptional target of PKA-CREB, regulates autophagic flux via interaction with the vacuolar ATPase

Sim Namkoong,[1] Kang Il Lee,[1] Jin I Lee,[1] Rackhyun Park,[1] Eun-Ju Lee,[2] Ik-Soon Jang,[3] and Junsoo Park[1],*

[1]Division of Biological Science and Technology; Yonsei University; Wonju, Korea; [2]Department of Obstetrics and Gynecology; Chung-Ang University School of Medicine; Seoul, Korea; [3]Division of Life Science; Korea Basic Science Institute; Daejeon, Korea

The PKA-CREB signaling pathway is involved in many cellular processes including autophagy. Recent studies demonstrated that PKA-CREB inhibits autophagy in yeast; however, the role of PKA-CREB signaling in mammalian cell autophagy has not been fully characterized. Here, we report that the integral membrane protein ITM2A expression is positively regulated by PKA-CREB signaling and ITM2A expression interferes with autophagic flux by interacting with vacuolar ATPase (v-ATPase). The *ITM2A* promoter contains a CRE element, and mutation at the CRE consensus site decreases the promoter activity. Forskolin treatment and PKA expression activate the *ITM2A* promoter confirming that ITM2A expression is dependent on the PKA-CREB pathway. ITM2A expression results in the accumulation of autophagosomes and interferes with autolysosome formation by blocking autophagic flux. We demonstrated that ITM2A physically interacts with v-ATPase and inhibits lysosomal function. These results support the notion that PKA-CREB signaling pathway regulates ITM2A expression, which negatively regulates autophagic flux by interfering with the function of v-ATPase.

Introduction

Macroautophagy (hereafter referred to as autophagy) is a protein degradation pathway that targets organelles and long-lived protein aggregates. Autophagy initiates with the formation of a phagophore, followed by expansion into an autophagosome, which fuses with a lysosome to form an autolysosome.[1] The contents sequestered in autolysosomes are degraded by lysosomal hydrolases at low pH. The conversion of autophagosomes into autolysosomes is inhibited by autophagy inhibitors, such as bafilomycin A_1 (BafA1) and chloroquine.[1,2] The dynamic process of autophagy is termed autophagic flux, which is important for analyzing autophagy.[3]

Autophagy can be induced by various stimuli, such as nutrient depletion (starvation), accumulation of damaged organelles, infection of cytoplasmic pathogen, hypoxia, and heat shock.[4,5] Each stimulus activates autophagy by using one of several different cell signaling pathways. Nutrient depletion results in the activation of AMP-dependent kinase (AMPK) and inactivation of MTOR (mechanistic target of rapamycin), which can activate the autophagy-initiating kinase ULK1 (Atg1 in yeast) in a phosphorylation-dependent manner.[6] In addition, MTOR complex 1 (MTORC1) phosphorylates ATG13 to inhibit autophagy induction.[7]

CREB (cAMP responsive element binding protein) regulates transcription of target genes in response to diverse stimuli such as peptide hormones, growth factors, and neuronal activity.[8] Typically, activation of a G protein-coupled receptor induces cAMP accumulation, which activates cAMP-dependent protein kinase (protein kinase A [PKA]). PKA activates CREB by

phosphorylating at serine residue 133.[9] This signaling cascade is called PKA-CREB signaling, and CREB also can be activated by a variety of protein kinases, such as MAPK (mitogen-activated protein kinase) and CAMK (calcium/calmodulin-dependent protein kinase) in a phosphorylation-dependent manner.[8]

In yeast, the inhibitory role of PKA-CREB signaling in autophagy has been clearly shown. PKA activation in yeast inhibited autophagy, and inactivation of the PKA pathway is sufficient to induce autophagy.[10] Moreover, PKA inhibits autophagosome formation by phosphorylating ATG1 and ATG13, which are conserved regulators of autophagy.[10-12] In mammalian cells, recent studies suggest that PKA-CREB signaling may negatively regulate autophagy; however, the detailed role of the PKA-CREB pathway in mammalian cell autophagy has not been fully identified.[13] Studies on the role of cAMP, an activator of PKA-CREB signaling, could elucidate the mechanism of PKA-CREB signaling in mammalian cell autophagy. cAMP has been reported to stimulate autophagy in rat livers; however, a recent study showed that bacteria can inhibit mammalian cell autophagy by generating cAMP.[13,14] Still, the mechanism of how PKA-CREB interacts with the molecular components of autophagy remains unknown.

ITM2A is a type II integral membrane protein that was initially identified as a candidate marker for chondro-osteogenic differentiation using cDNA library subtraction.[15] Several reports support the notion that ITM2A is involved in cell differentiation, though its effects depend on the cell type. ITM2A is expressed at sites of skeletal muscle formation, but its role in differentiation is not clear.[16] While ITM2A expression enhances myogenic differentiation of C2C12 cells, forced ITM2A expression inhibits chondrogenic differentiation of mesenchymal stem cells.[17,18] In addition, a recent report showed that ITM2A expression is regulated by the transcription factor GATA3, which is expressed exclusively in the T cell lineage. ITM2A overexpression in mouse T cells partially suppresses CD8 expression suggesting ITM2A is involved in T cell development.[19,20] Although several reports have shown that ITM2A is potentially involved in cell differentiation, the cellular function of ITM2A is not characterized. In this report, we show a novel role of ITM2A in autophagy. We showed that ITM2A expression is regulated by the PKA-CREB pathway. We also showed that ITM2A is involved in autophagic flux by interacting with v-ATPase, and ITM2A interaction with v-ATPase potentially contributes to the regulation of autophagy.

Results

ITM2A expression is regulated by the PKA-CREB pathway

In an attempt to identify the regulatory element involved in ITM2A expression, we analyzed the nucleotide sequence of ITM2A promoter with the Champion ChIP Transcription Factor Search Portal (Qiagen, Hilden, Germany) and found a putative CRE site in the ITM2A promoter sequence (**Fig. 1A**). To examine whether the CRE site is functional, we constructed a series of reporter plasmids that contained the −1,462 /+98 (−1.5 kb promoter), −1,030 /+98 (−1.0 kb promoter) and −529 /+98 (−0.5 kb promoter)

fragments relative to the transcription start site (TSS) of ITM2A, based on the Eukaryotic Promoter Database.[21] Because forskolin, a PKA activator, stimulates CREB (a CRE binding protein), we transfected HEK293 cells with reporter plasmids containing the ITM2A promoter regions and treated the cells with forskolin. While the control reporter (pGL2-basic) did not respond to the forskolin treatment, significant activation was observed with the reporter constructs containing ITM2A promoter regions (**Fig. 1B**). In addition, the relative luciferase activity in pGL2–1.5 transfected cells was significantly lower than pGL2–0.5 and pGL2–1.0 suggesting that there is a potential negative regulatory element between −1,462 and −1,030 (**Fig. 1B**). Because there were putative CRE (−30 to −24) and GATA (−256 to −253) elements within the ITM2A promoter, we generated constructs with mutations at the CRE and GATA sites to determine which element was functional (**Fig. 1A**). The reporter activity was significantly reduced with the ITM2A promoter containing 3 nucleotide changes at the CRE site (pGL2–0.5 CRE M2) (**Fig. 1C**). These results suggest that CRE and CREB regulate ITM2A expression.

CREB activation is mediated by multiple pathways, including the cAMP-PKA-CREB and PKC-MAPK pathways. Because forskolin activates the cAMP-PKA-CREB pathway, we tested whether PKA can activate the ITM2A promoter. Transient PKA expression activated the ITM2A promoter, and this activation was decreased with pGL2–0.5 CRE M2 (**Fig. S1**). To assess ITM2A expression by the cAMP-PKA-CREB pathway, we searched the GEO profiles database in NCBI using the keywords "ITM2A" and "PKA." The results showed that cAMP treatment increased ITM2A expression in the presence of wild-type PKA but not mutant PKA (**Fig. S2**).[22] To determine whether the PKC-MAPK pathway activates the ITM2A promoter, we treated cells with 12-O-tetradecanoylphorbol-13-acetate (TPA); TPA, however, did not activate the ITM2A reporter constructs or mutants (**Fig. S3**). These results collectively indicate that the ITM2A promoter is specifically activated by PKA-CREB signaling.

Because the ITM2A promoter is activated by the PKA-CREB pathway, we examined whether endogenous ITM2A expression is also regulated by the PKA-CREB pathway. We generated a rabbit polyclonal antibody against ITM2A and examined the expression of endogenous ITM2A by HEK293 cells after forskolin treatment. A western blot with the anti-ITM2A antibody revealed that forskolin treatment increased ITM2A expression up to fold4- (**Fig. 1D**). Next, we examined whether activated CREB interacts with the ITM2A promoter. HEK293 cells were either mock-treated or treated with forskolin, and a chromatin immunoprecipitation (ChIP) assay showed that phospho-CREB bound to the ITM2A promoter upon forskolin treatment (**Fig. 1E**). Finally, we examined whether ITM2A expression requires CREB protein. We silenced CREB expression with CREB siRNA, which reduced ITM2A expression, as assessed by semiquantitative RT-PCR and western blot. This result indicates that ITM2A expression requires CREB expression (**Fig. 1F**). Collectively, these results indicate that ITM2A expression is regulated by PKA-CREB signaling.
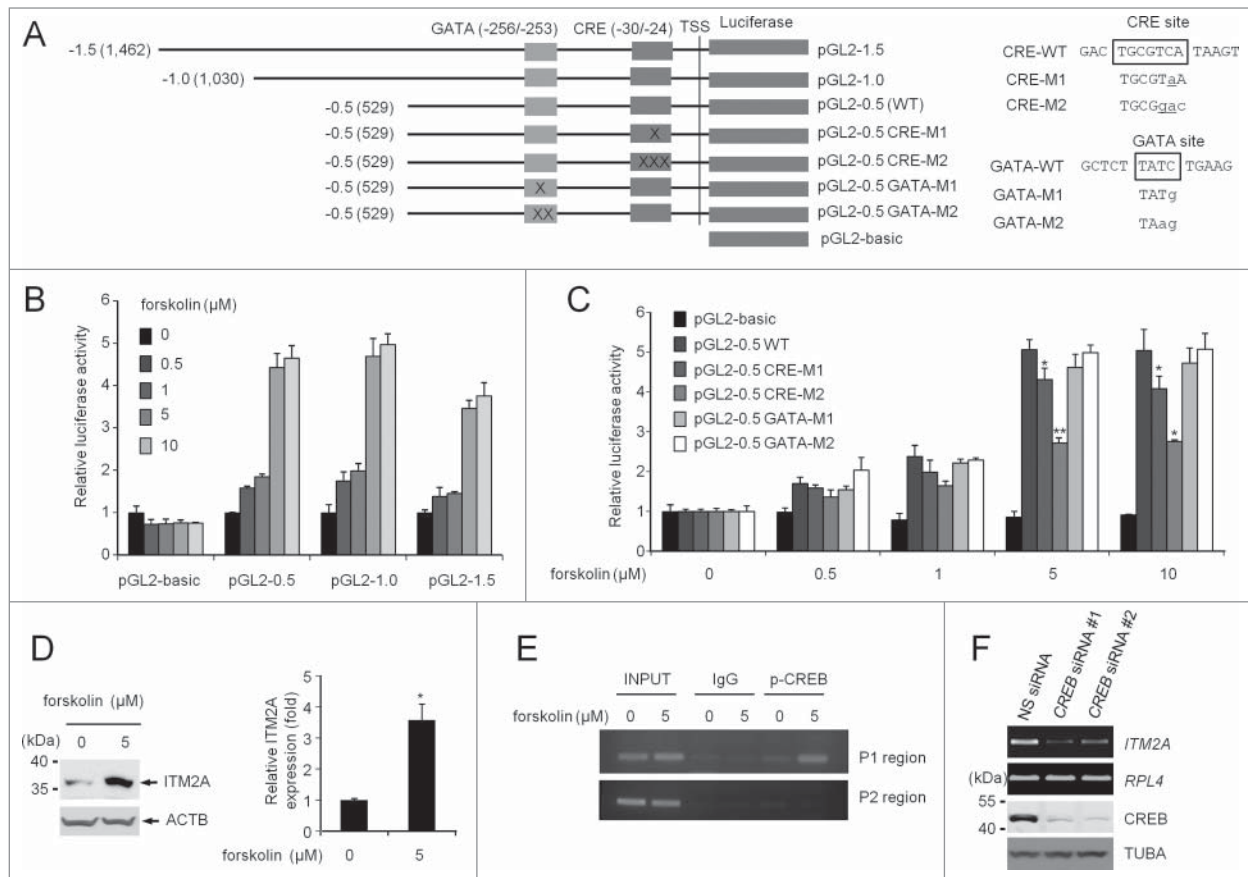
Figure 1. The *ITM2A* promoter is regulated by the PKA-CREB pathway. (**A**) Schematic diagrams of serial deletion constructs of the *ITM2A* promoter. The numbers to the left of each construct indicate the distance from the transcription start site (TSS). The predicted cis-elements (GATA, CRE) are indicated, and mutations in GATA or CRE are indicated with X's (left panel). Changed nucleotides in mutant constructs are indicated (right panel). (**B**) The *ITM2A* promoter is activated by forskolin treatment. HEK293 cells were transfected with reporter constructs. Twenty-four h after transfection, cells were treated with forskolin for 4 h, and luciferase activity was measured. Relative luciferase activity was normalized to renilla luciferase activity and is represented as a fold increase compared with the control. Experiments were performed in triplicate, and the standard deviation is shown. (**C**) CRE mutation reduces promoter activity. A luciferase assay was carried out with either wild-type promoter or mutant promoters. pGL2–0.5 wild type versus pGL2–0.5 mutant. *$P < 0.05$; **$P < 0.001$. (**D**) Forskolin induces ITM2A expression. HEK293 cells were treated with forskolin for 4 h, and cell lysates were subject to western blot with anti-ITM2A antibody. The bands were quantified and the fold activation is shown. 0 μM vs. 5 μM. *$P < 0.05$. (**E**) Phospho-CREB binds to the *ITM2A* promoter. HEK293 cells were treated with forskolin and a ChIP assay was performed with either normal IgG antibody or an anti-phospho-CREB antibody. (**F**) Reduced CREB expression decreased ITM2A expression. HEK293 cells were transfected with either nonspecific (NS) siRNA or *CREB* siRNA and ITM2A expression was measured by semiquantitative PCR.

ITM2A expression induced accumulation of autophagosomes

To investigate the cellular function of ITM2A, we examined the expression and subcellular localization of ITM2A along with numerous markers for cellular organelles, including EEA1 for early endosomes, and LAMP1 for lysosomes. ITM2A was overexpressed in HEK293 cells and immunostained with anti-ITM2A antibody and several other marker antibodies. Interestingly, confocal microscopy showed that ITM2A was expressed in HEK293 cells, and a portion of ITM2A colocalized with LAMP1 (**Fig. 2A**). We quantified the extent of colocalization and demonstrated that the colocalization of ITM2A and LAMP1 was significant (**Fig. S4**). We also observed the expression and cellular localization of endogenous ITM2A. In HEK293 cells, endogenous ITM2A is rarely detected under confocal microscopy

(**Fig. 2B**, **upper panel**). However, forskolin treatment elevates the expression of ITM2A in HEK293, and ITM2A is colocalized with the LAMP1 (**Fig. 2B**, **lower panel**). Moreover, we often observed abnormally enlarged lysosomes which expressed both ITM2A and LAMP1 (**Fig. 2B**, **lower panel**). These results suggest that ITM2A may be associated with lysosomes.

As ITM2A expression is activated by the PKA-CREB pathway and ITM2A is associated with the lysosomes, we further investigated the cellular function of ITM2A. Because PKA-CREB signaling is involved in autophagy, we examined whether ITM2A also functions in autophagy regulation. We generated HEK293 cells stably expressing ITM2A and the different clones showed variable expression levels of ITM2A. While 2 clones (#6 and #9) showed higher levels of expression of ITM2A, one
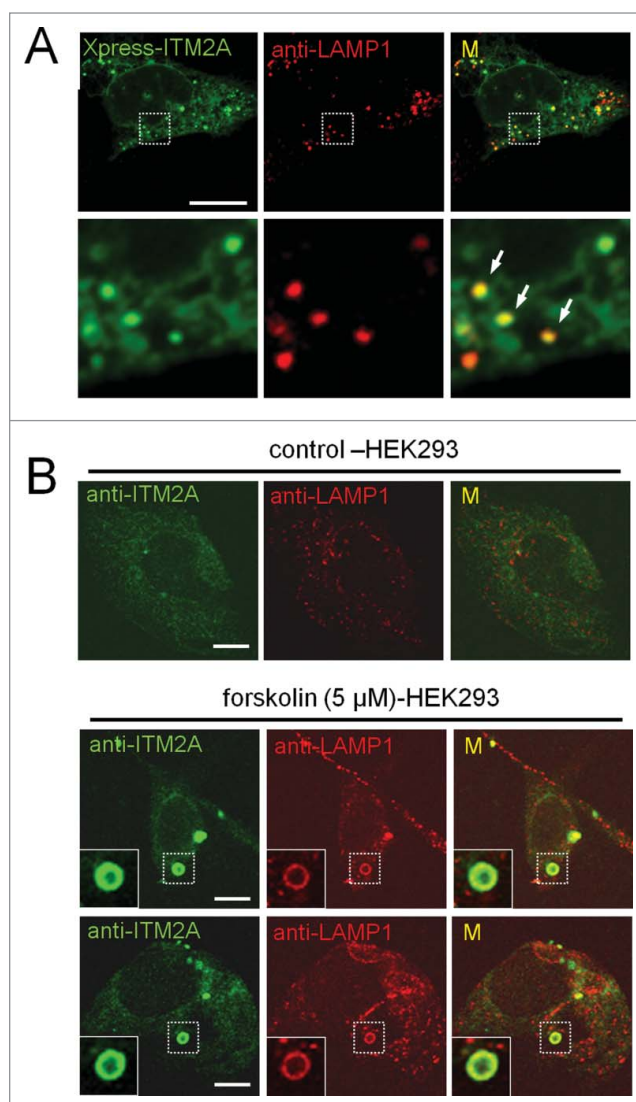
Figure 2. ITM2A localizes in the lysosomes. (**A**) Overexpressed ITM2A is colocalized with lysosomes. HEK293 cells were transfected with Xpress-ITM2A and cells were stained with anti-ITM2A antibody and anti-LAMP1 antibody (lysosome). The bottom panel depicts enlarged images of areas indicated in the top panel by white boxes. Bars: 10 μm. (**B**) ITM2A is colocalized with lysosomes by forskolin treatment in HEK293 (upper panel). HEK293 cells were incubated with either mock or forskolin (5 μM, 6 h), and cells were immunostained with anti-ITM2A antibody and anti-LAMP1 antibody. Bars: 10 μm. Top and bottom represent 2 different images of same sample (lower panel). Boxes denote enlarged regions.

clone (#1) rarely expressed ITM2A (**Fig. S5**). The cells expressing higher levels of ITM2A showed increased ratios of LC3B-II over LC3B-I as well as SQSTM1/p62 (**Fig. 3A**). Treatment with BafA1 also increased the level of ITM2A indicating that BafA1 affects the expression of ITM2A protein level (**Fig. 3A**). In addition, the transient expression of ITM2A results in the increased level of LC3B-II and SQSTM1 in a dose-dependent manner (**Fig. 3B**). We also tested the effect of ITM2A expression on SQSTM1 protein expression (**Fig. 3B**). Autophagy induction generally decreases the level of SQSTM1 protein. We

observed that ITM2A expression increases the level of SQSTM1, suggesting that ITM2A interferes with autophagic flux.

Next, we examined the subcellular localization of ITM2A and GFP-LC3B, an autophagosomal marker. HEK293 cells stably expressing GFP-LC3B were transfected with ITM2A, and we observed the cytoplasmic localization of GFP-LC3B. While GFP-LC3B was mainly localized in the nucleus after transfection of the control vector, transient ITM2A expression resulted in the formation of GFP-LC3B puncta in the cytoplasm (**Fig. 3C**). The accumulation of autophagosomes induced by ITM2A expression was extensive, and we compared the autophagosome patterns under starvation and with BafA1 treatment. The autophagosomes under starvation were relatively small and variable, while those formed with BafA1 treatment were relatively large. Autophagosomes formed by ITM2A expression were more similar to those formed by BafA1 treatment (**Fig. 3C**). We also examined the colocalization of GFP-LC3B with ITM2A. Although ITM2A does not completely colocalize with GFP-LC3B, the localization of ITM2A is closely localized to GFP-LC3B puncta in HEK293 cells (**Fig. 3D**). In addition, we transfected HEK293 cells with *ITM2A* and the examined the cellular localization of ITM2A and endogenous LC3. Autophagosomes accumulated in the transfected cells, and ITM2A is closely localized to LC3 puncta (**Fig. 3E**). We also observed the colocalization of GFP-LC3B with endogenous ITM2A in HeLa cells (**Fig. S6**). ITM2A is not colocalized with GFP-LC3B protein, however the endogenous ITM2A is often closely related with GFP-LC3B puncta (**Fig. S6**). These results suggest that ITM2A is involved in the accumulation of autophagosomes and closely related with autophagosomes.

ITM2A expression induces the accumulation of autophagosomes by interfering with autophagic flux

Because ITM2A expression induces the accumulation of autophagosomes, we sought to determine its role in autophagosome formation. We silenced endogenous *ITM2A* expression by using siRNA and examined the effect on autophagy. HeLa cells were transfected with either control siRNA or *ITM2A* siRNA, and cells were starved with EBSS to examine autophagy. While EBSS treatment (starvation) increased the conversion of LC3B-I into LC3B-II in HeLa cells with control siRNA, silencing of *ITM2A* did not change the ratio of LC3B-II over LC3B-I with *ITM2A* siRNA under starvation (**Fig. 4A**). Next we silenced *ITM2A* and treated with BafA1 to block autophagic flux (**Fig. 4B**). As we observed previously (**Fig. 3A**), BafA1 treatment increases the level of ITM2A protein. Treatment of BafA1 is known to increase the ratio of LC3B-II over LC3B-I by blocking autophagic flux, and we observed this here as well (**Fig. 3A**; **Fig. 4B**). Silencing of *ITM2A* expression results in a significant decrease in the ratio of LC3B-II over LC3B-I. We also observed the effect of SQSTM1 expression when *ITM2A* expression is silenced. Interestingly, SQSTM1 expression levels were decreased in BafA1 and *ITM2A* siRNA treatment. Thus, ITM2A overexpression and silencing had profound and reciprocal effects on autophagy indicating an important role for ITM2A in autophagy.
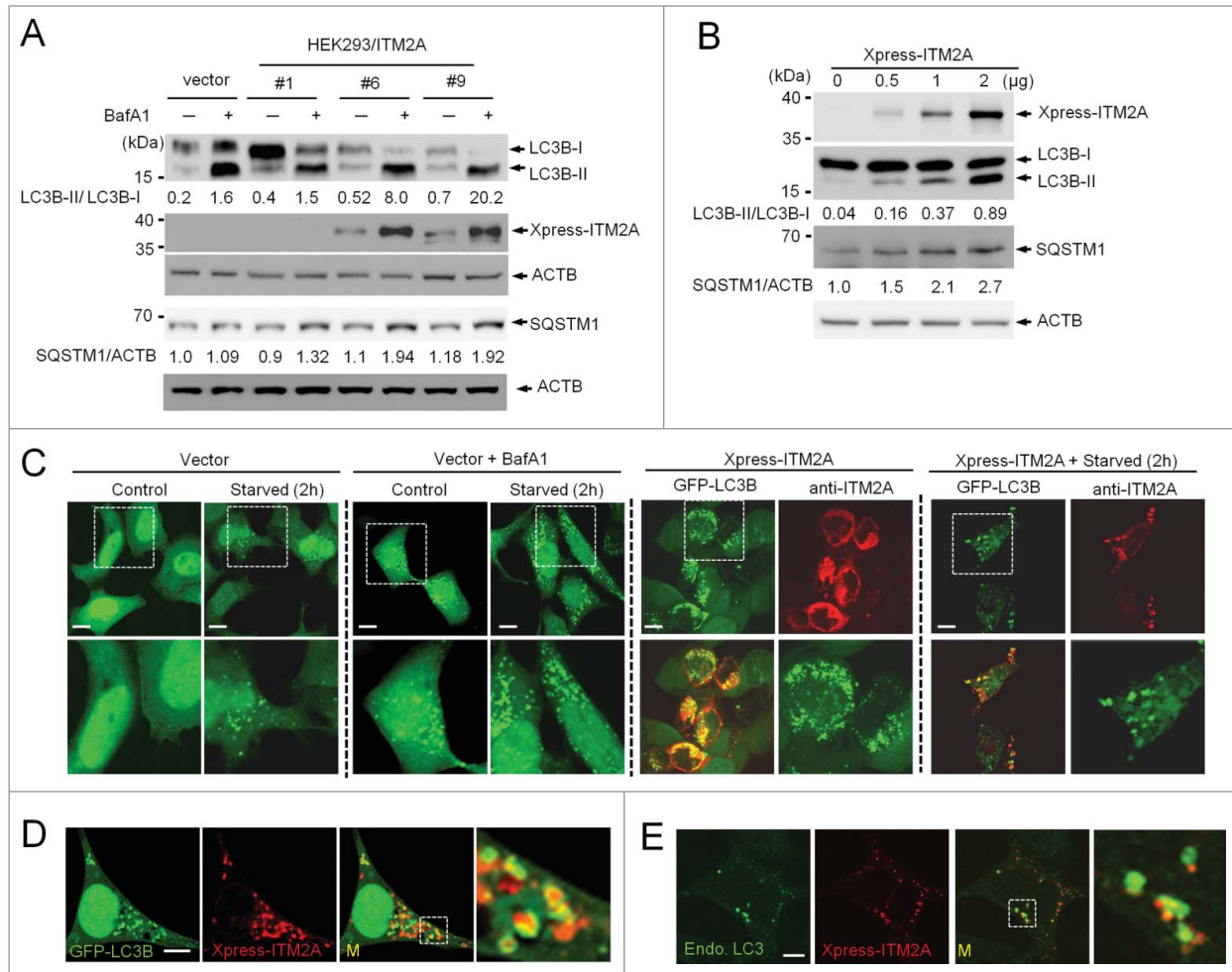
Figure 3. ITM2A expression results in the accumulation of autophagosomes. (**A**) Elevated level of ITM2A expression increased the LC3B-II/LC3B-I ratio. HEK293 cells stably expressing Xpress-ITM2A were incubated in the presence or absence of BafA1 and the cell lysates were subject to western blot with anti-LC3 antibody and anti-SQSTM1 antibody. LC3B-II/LC3B-I ratios and the level of SQSTM1 (the ratio of SQSTM1/ACTB) are indicated. (**B**) Overexpressing ITM2A increased the level of LC3B-II and SQSTM1. HEK293 cells were transfected with a plasmid encoding Xpress-ITM2A, and the cell lysates were subject to western blot with the indicated antibody. (**C**) Overexpressing ITM2A induces autophagosome accumulation in HEK293 cells. HEK293 cells stably expressing GFP-LC3B were transfected with either vector or a plasmid encoding ITM2A. Twenty-four h after transfection, cells were fixed and stained with anti-ITM2A antibody. Control cells were either mock-treated or starved in EBSS medium for 2 h in the presence or absence of BafA1 (100 nM). ITM2A transfected cells were either mock-treated or starved in EBSS medium. Bars: 10 μm. (**D**) ITM2A expression is closely associated with the autophagosome. HEK293 cells stably expressing GFP-LC3B were transfected with the plasmids encoding Xpress-ITM2A (red). Bars: 10 μm. (**E**) ITM2A is colocalized with the endogenous LC3. The HEK293 cells were transfected with plasmid encoding Xpress-ITM2A and immunostained with anti-LC3 (green) and anti-Xpress (ITM2A, red). Bars: 10 μm.

Next, we examined the effect of *ITM2A* silencing on the formation of autophagosomes. HeLa cells were transfected with siRNA and mRFP-GFP-LC3B reporter construct (tfLC3) with a time interval (24 h), and the cells were treated with mock, starvation, or BafA1 conditions. Unexpectedly, enlarged agglomerations of vesicles were formed by *ITM2A* silencing, and these agglomerations disappeared upon BafA1 treatment (**Fig. 4C**). Immunostaining with anti-LAMP1 antibody revealed that these *ITM2A* silencing-dependent agglomerations were also expressed with LAMP1 (GFP-LC3B^{+}, LAMP1^{+}) (**Fig. 4D**). These results collectively indicate that the silencing of ITM2A expression deregulates autophagy (**Figs. 4A-D**).

Autophagosomes can accumulate in 2 ways, either by inducing autophagy or instead by blocking autophagic flux.[1] The latter occurs because autophagosomes that normally fuse with lysosomes to form autolysosomes during autophagic flux now remain as autophagosomes and begin to accumulate. To examine the role that ITM2A plays during autophagic flux, we used the mRFP-GFP-LC3B reporter construct (tfLC3), which appears red when autolysosomes form.[23] Starvation for 2 h induced red puncta in the cytoplasm, indicating autolysosome maturation (Fig 5A, **ii**). BafA1 treatment, however, induces yellow puncta, indicating that autolysosome formation is blocked by BafA1 treatment (**Fig. 5A**, **iii**). Next, we examined the autophagic flux
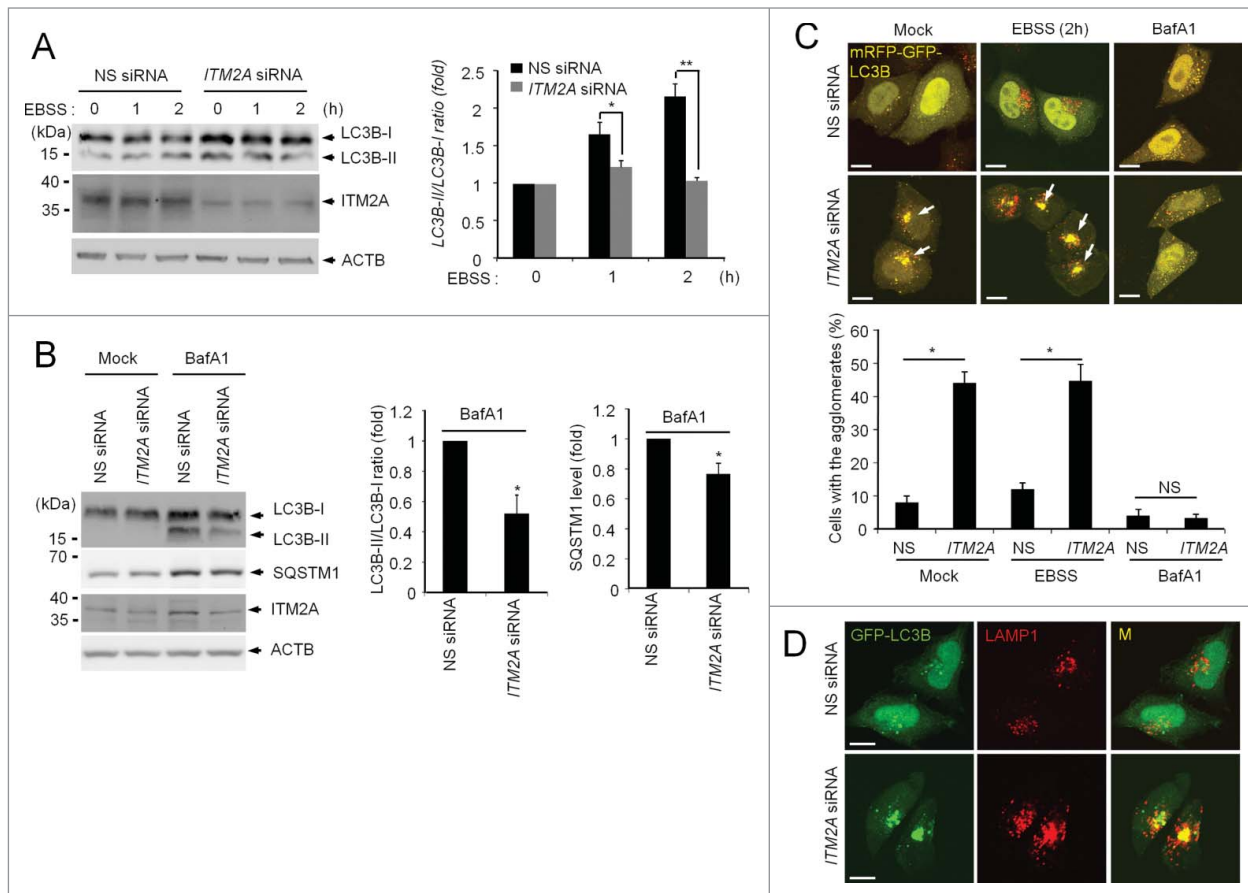
Figure 4. The silencing of ITM2A expression deregulates autophagy (**A**) Silencing *ITM2A* deregulates autophagy. HeLa cells were transfected with either nonspecific (NS) siRNA or *ITM2A* siRNA. Forty-eight h after transfection, cells were starved with EBSS for the indicated times, and the cell lysates were subjected to western blot with the indicated antibodies (left panel). The relative ratio of LC3B-II over LC3B-I (fold) was quantified (right panel). The experiments were repeated 3 times, and representative data are shown. 0 h vs. indicated times. NS siRNA vs. *ITM2A* siRNA. *$P < 0.05$; **$P < 0.005$. (**B**) Silencing *ITM2A* interferes with autophagic flux. HeLa cells were transfected with siRNA and cells were incubated in the presence or absence of BafA1 (100 nM, 4 h). The relative ratio of LC3B-II over LC3B-I (fold) and SQSTM1 were quantified (right panel). NS siRNA versus *ITM2A* siRNA. *$P < 0.05$. Bars: 10 μm. (**C**) Silencing *ITM2A* results in enlarged agglomerations of vesicles. HeLa cells were transfected with siRNA and the mRFP-GFP-LC3B reporter construct (tfLC3) with a time interval (24 h), and the cells were treated with mock, starvation or BafA1 conditions (upper panel). The number of the cells with the aggregates was counted using a fluorescence microscope (N=150). Control vector vs. *ITM2A* siRNA. *$P < 0.05$; NS significant. Bars: 10 μm. (**D**) Enlarged vesicles colocalize with LAMP1 protein. HeLa cells were transfected with siRNA and GFP-LC3B with a time interval (24 h), and the cells were immunostained with anti-LAMP1 antibody. Bars: 10 μm.

with ITM2A expression. When we observed autophagic flux upon ITM2A expression, ITM2A expression induces yellow puncta, and the patterns are similar to that of BafA1 treatments (**Fig. 5A**, **iv**). ITM2A expression also interferes with autolysosome maturation even under starvation conditions (**Fig. 5A**, **v**). These results indicate ITM2A interferes with autophagic flux by blocking the formation of a mature autolysosome (**Figs. 5A and B**).

The fusion of autophagosome with lysosomes results in the formation of a mature autolysosome. Since we show that ITM2A blocks the formation of a mature autolysosome, we examined whether ITM2A interferes with the fusion of autophagosome with lysosome. Because GFP-LC3B is quenched by low lysosomal pH, we used mRFP-LC3B for the detection of autophagic vacuoles including autophagosomes and autolysosomes. HEK293 cells were transfected with the plasmid encoding mRFP-LC3B in the presence or absence with the plasmid encoding ITM2A, and cells were incubated in either DMEM (mock) or EBSS (starvation). Control cells subjected to starvation conditions resulted in the formation of mRFP-LC3B puncta. We found that many of these puncta coincided with LAMP1 expression suggesting that the puncta were mature autolysosomes. However when ITM2A is overexpressed, we observed that many of the mRFP-LC3B puncta were not LAMP1-positive indicating that ITM2A may be interfering with the formation of autolysosomes (**Fig. 5C**). In addition, the transient expression of ITM2A increased the total level of GFP-LC3B suggesting that ITM2A blocked the degradation of the autophagic degradation of GFP-LC3B (**Fig. 5D**). These results collectively indicate that ITM2A may inhibit autophagic flux by interfering with fusion of autophagosomes with lysosomes.
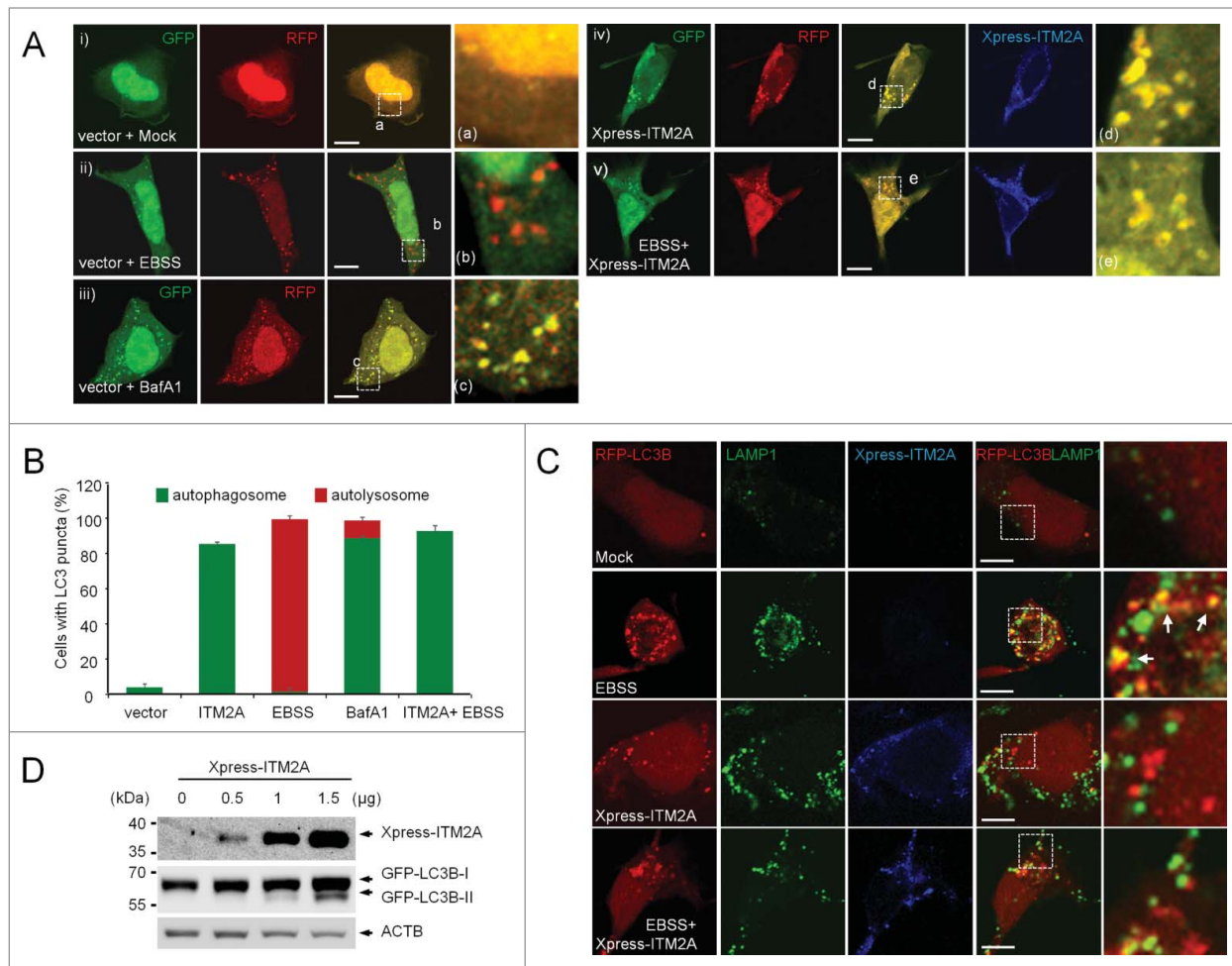
Figure 5. ITM2A expression interferes with autophagic flux. (**A**) HEK293 cells expressing mRFP-GFP-LC3B protein were transfected with either vector or the plasmid encoding ITM2A. Twenty-four h after transfection, cells were fixed and stained with an anti-ITM2A antibody. Control cells were either mock-treated or starved in EBSS medium for 3 h in the presence or absence of BafA1 (100 nM, 4 h). Bars: 10 μm. (**B**) Quantification of cells with either autophagosomal LC3 puncta or autolysosomal LC3 puncta (N = 300). (**C**) HEK293 cells were transfected with plasmid encoding mRFP-LC3B with either vector (first and second row) or the plasmid encoding ITM2A (third and fourth row), and subjected to either mock-treatment (first and third rows) or starved in EBSS medium (second and fourth rows) for 2 h, and stained with an anti-LAMP1 antibody and an anti-ITM2A antibody. (**D**) Overexpression of ITM2A increases the level of LC3B. HEK293 cells were transfected with the plasmid encoding GFP-LC3B (0.5 μg) in combination with the plasmid encoding Xpress-ITM2A (0, 0.5, 1 or 1.5 μg). Cell lysates were subject to western blot with the indicated antibodies.

ITM2A interacts with v-ATPase

Since ITM2A inhibits autophagic flux, we wanted to further examine the mechanism of inhibition. We searched the STRING v9.1 protein-protein interaction network, and found that ATP6V0A4/v-ATPase a4 was a potential binding partner.[24] To examine the interaction between ITM2A and ATP6V0A4, we performed a coimmunoprecipitation assay with endogenous ITM2A and endogenous ATP6V0A4. We immunopurified ITM2A protein with an anti-ITM2A antibody, and detected the bound ATP6V0A4 by anti-ATP6V0A4 antibody. The binding assay showed that ITM2A protein interacts with ATP6V0A4 tightly (**Fig. 6A**). We confirmed the interaction between ITM2A and ATP6V0A4 by the transiently expressing ITM2A and His-ATP6V0A4 (**Fig. 6B**). Since ATP6V0A4 is only one member of the v-ATPase a family, we assessed the interaction of ITM2A

with ATP6V0A1/v-ATPase a1, the more widely expressed form of the v-ATPase a family (**Fig. 6C**, right panel; **Fig. S7**). The binding assay showed that HA-ITM2A also interacts with endogenous ATP6V0A1 (**Fig. 6C**). To see if this interaction was specific for the v-ATPase a family, we also examined the interaction between ITM2A and ATP6V1B1 and ATP6V1B2, and we did not detect their interaction (data not shown). These results provide evidence for a specific interaction between ITM2A and the v-ATPase a family.

To investigate the interaction between ITM2A and v-ATPase, we assessed the subcellular localization of ITM2A and ATP6V0A4. HEK293 cells were transfected with plasmids encoding ATP6V0A4 in the presence or absence of ITM2A. ITM2A colocalized with ATP6V0A4, and the colocalization and the binding between ITM2A and ATP6V0A4 were not affected
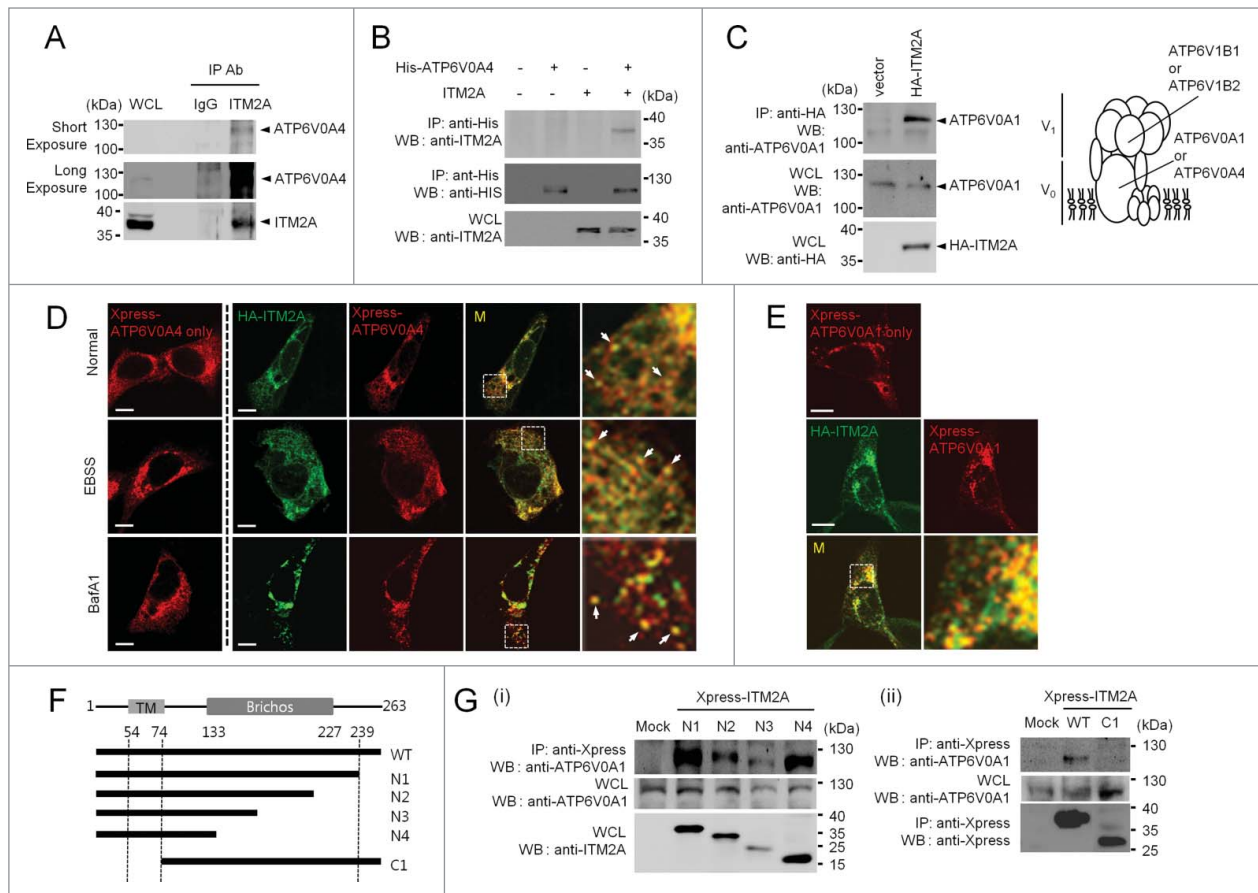
Figure 6. ITM2A interacts with v-ATPase. (**A**) Interaction between endogenous ITM2A and endogenous ATP6V0A4. HeLa cells were immunoprecipitated with either normal IgG or an anti-ITM2A antibody, followed by immunoblotting with an anti-ATP6V0A4 antibody (upper and middle panels) or anti-ITM2A antibody (lower panel). WCL, whole cell lysates. (**B**) Interaction between ITM2A and ATP6V0A4. HEK293 cells were transfected with HA-ITM2A, His-tagged ATP6V0A4 (His-ATP6V0A4) or both. ATP6V0A4 protein was immunopurified with an anti-His antibody and immunoprecipitates were immuno-blotted with an anti-ITM2A antibody. (**C**) Interaction between ITM2A and endogenous ATP6V0A1. HEK293 cells were transfected with HA-ITM2A, and HA-ITM2A was immunopurified to examine the interaction with endogenous ATP6V0A1 (left). Simplified figure of v-ATPase complex is shown and ATP6V0A1, ATP6V0A4, and ATP6V1B1/ATP6V1B2 are indicated (right). (**D**) ITM2A is colocalized with ATP6V0A4. HEK293 cells were transfected with plasmid encoding Xpress-ATP6V0A4 in the presence or absence of plasmid encoding ITM2A. Cells were mock-treated, starved for 2 h or incubated with BafA1 (100 nM, 4 h) and immunostained with anti-Xpress (red) or anti-ITM2A (green) antibodies. Bars: 10 μm. (**E**) ITM2A is colocalized with ATP6V0A1. HEK293 cells were transfected with plasmid encoding Xpress-ATP6V0A1 in the presence or absence of plasmid encoding ITM2A. Bars: 10 μm. (**F**) Schematic diagram of ITM2A and its deletion mutants (N1 to N4, C1). Numbers correspond to the amino acid sequence. TM, transmembrane domain. (**G**) Identification of the region of ITM2A required for v-ATPase interaction. (i) HEK293 cells were transfected with Xpress-tagged ITM2A mutants (N1, N2, N3, N4), and Xpress-ITM2A mutants were immunopurified with anti-Xpress antibody. The immunoprecipitates were probed with anti- ATP6V0A1 antibody. (ii) HEK293 cells were transfected with Xpress-ITM2A wild type (WT) or Xpress-tagged ITM2A C1 (C1). Xpress-ITM2A proteins were immunopurified with an anti-Xpress antibody and immunoprecipitates were immunoblotted with an anti-ATP6V0A1 antibody.

by either the starvation or the BafA1 treatment (**Fig. 6D; Fig. S8**). In addition, ITM2A also colocalized with ATP6V0A1 (**Fig. 6E**).

Because ITM2A interacts with v-ATPase, we determined which ITM2A domain is required for the interaction. ITM2A has 2 functional domains, the transmembrane domain (amino acids 54 to 74) and the putative brichos domain (amino acids 133 to 227). We generated ITM2A constructs containing truncated forms of ITM2A (ITM2A N1, N2, N3, N4, and C1) based on the functional domains, and examined the interaction with ATP6V0A1. HEK293 cells were transfected with plasmids encoding either Xpress-

ITM2A or Xpress-ITM2A mutant. Forty-eight h after trans-fection, Xpress-ITM2A protein was immunoprecipitated and the immunoprecipitates were probed with an anti-ATP6V0A1 antibody. The coimmunoprecipitation assay revealed that ITM2A WT, N1, N2, N3, and N4 interact with ATP6V0A1 suggesting that the N terminus (amino acids 1 to 133) is suf-ficient for binding (**Fig. 6G, I**). In addition, we examined whether ATP6V0A1 was associated with the ITM2A C1 mutant. A coimmunoprecipitation with ITM2A C1 and v-ATPase showed that ITM2A C1 does not interact with ATP6V0A1 and ATP6V0A4 indicating that the N terminus is required for binding with v-ATPase (**Fig. 6G, ii; Fig. S9**).

The interaction between ITM2A and v-ATPase is required for the accumulation of autophagosomes by ITM2A

We examined the effect of truncated ITM2A mutants on autophagosome formation. ITM2A mutants (N1 to N4) which interact with v-ATPase induced the accumulation of autophagosomes (**Figs. 7A and B; Fig. S10**). On the other hand, ITM2A C1 expression did not induce autophagosome accumulation. In addition, ITM2A C1 did not increase the level of LC3B-II (**Fig. 7C; Fig. S10**). These results indicate that N-terminal domain of ITM2A is required for the accumulation of autophagosomes.

Several reports suggest that v-ATPase is responsible for acidifying the autophagic vacuole and that BafA1 inhibits v-ATPase.[2] Because ITM2A interacts with v-ATPase, we examined whether lysosomal function was affected by ITM2A expression. GFP-LC3B cells were transfected with the plasmid encoding ITM2A and starved for 3 h. Later, the cells were stained with Lyso-Tracker Red to examine lysosomal function. LysoTracker Red dyes accumulated in cellular organelles, which are acidic. ITM2A expression reduced the LysoTracker Red spots indicating that ITM2A interferes with lysosomal function (**Fig. 7D**, left panel).

To investigate the significance of our results, we analyzed the number of LysoTracker Red spots using cells expressing wild-type ITM2A or N-terminal truncated ITM2A C1. While wild-type ITM2A significantly reduced the number of LysoTracker Red spots, ITM2A C1 that cannot interact with v-ATPase remained similar to control levels (**Fig. 7D**, right panel). To confirm whether ITM2A affected lysosomal pH, we used a LysoSensor dye. Overexpression of wild-type ITM2A significantly increased the lysosomal pH, however ITM2A C1 did not change the lysosomal pH (**Fig. 7E**). These results suggest that ITM2A suppresses the acidification of subcellular organelles through interactions with v-ATPase.

Discussion

Here we demonstrate that ITM2A is induced by the PKA-CREB signaling pathway. We first analyzed the *ITM2A* promoter sequence, and determined that the *ITM2A* promoter contains a CRE element. We then examined the relationship between ITM2A expression and PKA-CREB signaling. ITM2A
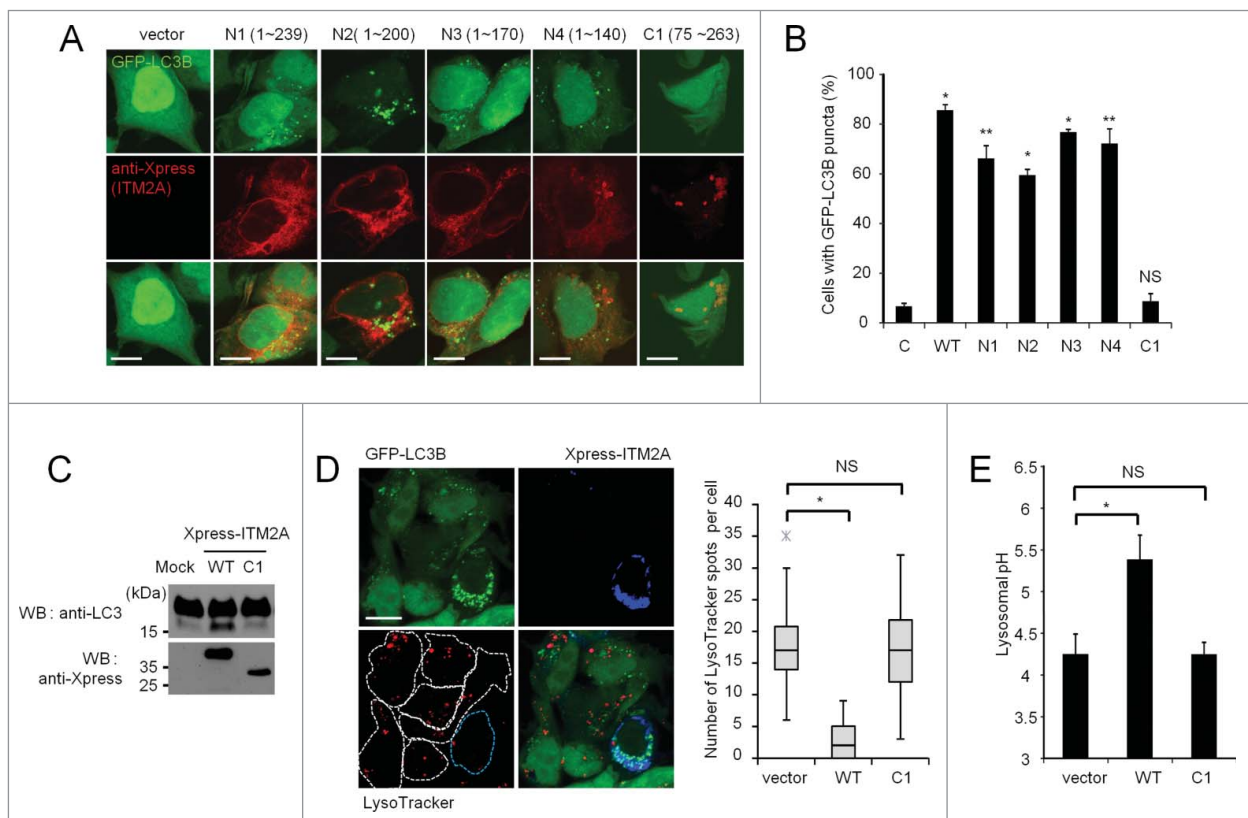
Figure 7. ITM2A interferes with lysosomal function. (**A**) The N-terminal domain of ITM2A is required for autophagosome formation. ITM2A deletion mutants were expressed in GFP-LC3B cells and stained with anti-Xpress antibody. Bars: 10 μm. (**B**) The number of GFP-LC3B dot-positive cells (N > 5) was counted using a fluorescent microscope (N=300). Control vector versus ITM2A mutant. *$P < 0.001$; **$P < 0.005$; NS, not significant. (**C**) ITM2A C1 did not increase the LC3B-II/LC3B-I ratio. HEK293 cells were transfected with vector, ITM2A WT, or ITM2A C1 and the cell lysates were subjected to western blot with anti-LC3 antibody. (**D**) ITM2A interferes with the acidification of lysosomes. GFP-LC3B cells were transfected with plasmid encoding ITM2A. Twenty-four h after transfection, cells were starved for 3 h and stained with LysoTracker Red dye (left panel). The number of LysoTracker Red spots was counted using a fluorescence microscope (right panel). N = 50 , *$P < 10^{-19}$; NS, not significant. Bars: 10 μm. (**E**) Lysosomal pH values were measured using LysoSensor Yellow/Blue-dextran. N = 3 , *$P < 0.05$; NS, not significant.

expression is induced by both forskolin treatment and forced PKA expression, and depleting *CREB* with siRNA attenuates ITM2A expression. Next, we examined the cellular function of ITM2A. Because we observed the accumulation of autophagosomes induced by ITM2A expression, we hypothesized that ITM2A is involved in autophagy. Our hypothesis was supported by the following evidence: HEK293 cells stably expressing ITM2A showed an increase in the LC3B-II/LC3B-I ratio, and the silencing of *ITM2A* interferes with the autophagy process under starvation conditions. In particular, we found that ITM2A expression interferes with autolysosome formation, indicating that ITM2A interferes with autophagic flux. To identify the mechanism by which ITM2A inhibits autophagic flux, we searched the ITM2A binding partners and identified v-ATPase by *in silico* analysis. ITM2A interacts tightly with v-ATPase and colocalizes with v-ATPase in the cytoplasm. v-ATPase acidifies intracellular organelles. Thus, the interaction between v-ATPase and ITM2A attenuates lysosome function and suppresses autolysosome formation. These results show that PKA-CREB signaling interferes with autophagic flux by regulating ITM2A, which interacts with v-ATPase.

v-ATPase acidifies organelles and is required for the autophagy process. For this reason, v-ATPase inactivation by mutation or an inhibitor such as BafA1 results in attenuated autophagy.[2,25] In this study, ITM2A provided similar results and ITM2A expression resulted in enlarged autophagosomes and inhibited autophagic flux. In addition, we showed that ITM2A interacts with v-ATPase and inhibits autophagic flux, indicating that ITM2A interferes with v-ATPase function. Our speculation is also supported by a decrease in LysoTracker Red spots and the increase of lysosomal pH following ITM2A expression. For this reason, the elevated expression of ITM2A can be considered a novel method to inhibit v-ATPase.

ITM2A mutants (N1 to N4) containing the transmembrane domain interacted with v-ATPase, whereas the ITM2A C1 mutant, which is devoid of the transmembrane domain, did not interact with v-ATPase. Thus, we concluded that N-terminal domain of ITM2A is required for the interaction between ITM2A and v-ATPase. In addition, ITM2A interacts with v-ATPase a subunits such as ATP6V0A1 or ATP6V0A4 but not ATP6V1B1 or ATP6V1B2. As v-ATPase a and v-ATPase B are different families of v-ATPase, we speculate that this distinction is caused by differences in amino acid sequences. The amino acid sequences of ATP6V0A1 are homologous with ATP6V0A4, whereas those of ATP6V1B1 and ATP6V1B2 are not as related to ATP6V0A4.

Silencing *ITM2A* expression by siRNA produced some interesting results. Reduced endogenous ITM2A expression attenuated autophagy under starvation. Normally, the LC3B-II level under starvation is increased, indicating active autophagy. However, silencing *ITM2A* expression attenuates the change in the ratio of LC3B-II/LC3B-I expression. These results suggest that ITM2A has a negative role in regulating autophagy. Moreover, the silencing of *ITM2A* interferes with the function of BafA1, which blocks autophagic flux. The level of ITM2A protein was elevated by BafA1 treatment, and the silencing of *ITM2A*

decreased LC3B-II/LC3B-I ratio as well as protein levels of SQSTM1. Namely, *ITM2A* silencing attenuated the inhibitory effect on autophagic flux of BafA1. These results suggest that ITM2A is possibly involved in the function of BafA1 by regulating v-ATPase.

Based on our results, ITM2A inhibits the autophagic flux by regulating the fusion of autophagosome with lysosome (**Fig. 8**). When the expression level of ITM2A is increased, ITM2A colocalizes with lysosomes, and the lysosome rarely colocalizes with autophagosomes (**Figs. 2A and B; Fig. 5C**). Enhanced expression of ITM2A by forskolin or transient expression formed abnormally enlarged lysosomes (ITM2A^{+}, LAMP1^{+}, GFP-LC3B^{-}) by regulating the lysosomal pH (**Figs. 2A and 2B; Fig. 7E**). Thus, ITM2A expression results in the accumulation of autophagosomes and lysosomes (**Fig. 8B**). In contrast, the silencing of *ITM2A* attenuates the inhibitory effect of ITM2A on v-ATPase, and results in the formation of incomplete enlarged autolysosomes (ITM2A^{-}, LAMP1^{+}, GFP-LC3B^{+}) (**Figs. 4C and D**). Similar agglomerated vesicles were also found when autophagic flux was activated by the overexpression of UVRAG.[26] Moreover, BafA1 treatment decreased the number of enlarged autolysosomes in *ITM2A* silenced cells. One possible explanation for this is that BafA1 can decrease v-ATPase activity and inhibit the fusion of autophagosomes and lysosomes, resulting in a loss of enlarged autolysosomes (**Figs. 4C and D**). However, it is still controversial whether v-ATPase is involved in the fusion of autophagosomes with lysosomes.[2,27] In this report, we focus on the inhibition of autophagy flux by ITM2A by interacting with v-ATPase, however we speculate that ITM2A has additional roles in regulating the fusion of autophagosomes with lysosomes.

Several reports suggest that PKA signaling inhibits autophagy. In yeast, the Ras-PKA signaling pathway inhibits an early step in the autophagy process, and the PKA as well as the TOR pathways regulate Atg1 and Atg13 by phosphorylation.[10,12] However, the relationship between CREB and autophagy has not been as clearly studied in the mammalian systems as it has in yeast. Here, we showed that ITM2A is a direct transcriptional target of CREB that interferes with the later stage of autophagy. Overall, our data suggest that PKA-CREB signaling in mammalian cells negatively affects autophagy. We attempted to examine the autophagy process by PKA-CREB in the presence or absence of ITM2A, however we did not find a clear difference (data not shown). We assume that multiple autophagy pathways including the early step are inhibited by the PKA pathway, and the inhibition of later steps such as autolysosome formation is a kind of a double check to block autophagy.

Several reports demonstrated that ITM2A is involved in cell differentiation. Similarly, autophagy has a critical role in cell differentiation, and knocking out autophagy regulators such as *Atg5* or *Atg7* has led to various differentiation abnormalities.[28] Overexpressing ITM2A enhances myotube differentiation of C2C12 myoblast cells and knocking out *Atg7* results in muscle atrophy and muscle loss during denervation and fasting.[18,29] On the basis of our findings regarding the role of ITM2A in autophagy and previous results, we speculate that ITM2A regulates cell differentiation by regulating autophagy. Many positive or negative
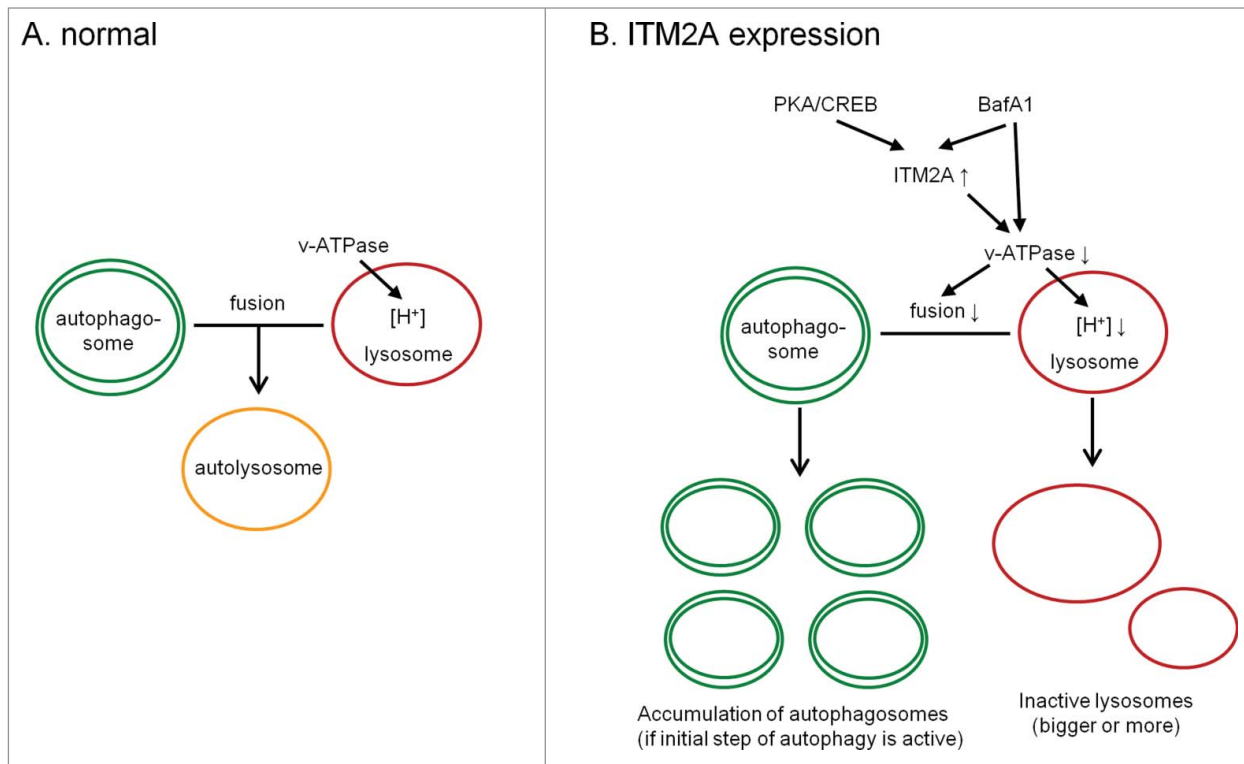
Figure 8. A proposed hypothesis of the cellular pathway involving ITM2A and v-ATPase regulating the acidification of autophagosomes and autophagic flux. (**A**) v-ATPase is involved in the transport of hydrogen ion, and also involved in the fusion of autophagosomes with lysosomes. (**B**) Upregulation of ITM2A expression inhibits the transport of hydrogen ion by interacting with the v-ATPase. Inactivation of the v-ATPase inhibits the fusion of autophagosomes with lysosomes, and contributes to the accumulation of autophagosomes and lysosomes.

regulators of autophagy participate in cell remodeling, and ITM2A regulating autophagy could affect cell differentiation. Further research will be required to determine relationship between autophagy regulation by ITM2A and cell differentiation.

Materials and Methods

Cell culture and reporter assay

HEK293 and HeLa cells were grown in DMEM medium (Welgene, LM001–05) supplemented with 10% fetal bovine serum (Gibco, 26140). A HEK293 stable cell line expressing GFP-LC3B was generated as described previously.[30] The GFP-LC3B plasmid was provided by T. Yoshimori (Osaka University, Japan).[31] HEK293 cells were transfected using lipofectamine 2000 (Invitrogen, 11668). For the reporter assay, cells were seeded in 24-well plates in DMEM 18 h before transfection. Typically, 0.5 μg of total DNA was transfected in each well, and each assay was normalized with renilla luciferase. To examine the cell signaling pathways, HEK293 cells were treated with forskolin (Sigma, F6886), TPA (Sigma, P1585) and BafA1 (Sigma, B1793).

cDNA cloning and reporter plasmid construction

Reverse Transcription - Polymerase Chain Reaction (RT-PCR) was used to amplify the entire coding region of *ITM2A* from

HEK293 RNA using the 5′ primer ATG GTG AAA ATC GCC TTC AAT AC and the 3′ primer TTA ATC TTG ACA GAT CTT GGT CTC AAC. The amplified cDNA fragments were cloned into pcDNA4/HisMax (Invitrogen, K864–20) to encode Xpress tagged ITM2A (Xpress-ITM2A) and completely sequenced. After sequencing, cDNA for *ITM2A* was subcloned into pcDNA3/HA plasmids. In the same way, v-ATPase (*ATP6V0A4*) was amplified using 5′ primer ATG GTG TCT GTG TTT CGA AGC and 3′ primer CTA CTC CTC GGC TGT GCC ATC from HeLa cDNA and cloned into pcDNA4/HisMax. The *ITM2A* promoter region (-1,462 /+98) was amplified from HEK293 genomic DNA using 5′ primer TGG CCC TAA GTA AGG CAC AG and 3′ primer GTA AGG CGC TGC TGG AAT C. The amplified fragments were initially cloned into the pTOP TA V2 vector (Enzynomics, EZ011). Each reporter plasmid construct (1.5 kb, 1.0 kb and 0.5 kb) was amplified and subsequently subcloned into pGL2-basic vector (Promega, E1641). Point mutants of the *ITM2A* promoter were generated using the QuikChange site-directed mutagenesis kit (Stratagene, #200518), and each mutant was completely sequenced to verify the presence of the intended mutation and the absence of any others.

Immunoprecipitation and western blotting

For immunoprecipitation, cells were harvested and resuspended in lysis buffer (150 mM NaCl, 50 mM HEPES, pH 7.5, 1% NP40 [Sigma, I8896]) containing a protease inhibitor

cocktail (Roche, 11697498001). Immunoprecipitated proteins from precleared cell lysates were used for immunoblotting. For protein immunoblot analysis, polypeptides in whole cell lysates were resolved by SDS-PAGE and transferred to nitrocellulose membrane filters. Proteins were detected with a 1:2000 or 1:5000 dilution of primary antibody using an enhanced chemiluminescence (ECL) system. The images were acquired using Chemidoc-it 410 imaging system (UVP, Upland, CA) and LAS4000 system (GE Healthcare, Uppsala, Sweden). Glutathione S-transferase (GST)-ITM2A amino-terminal fragment (amino acid 1 to 120) fusion protein was used as a source antigen for the anti-ITM2A antibody. The following primary antibodies were used: anti-CREB (Cell Signaling Technology, 9197), anti-phospho-CREB (Cell Signaling Technology, 9198), anti-LC3 (Novus Biologicals, NB100–2220), anti-ATP6V0A4 (Aviva Systems Biology, OAAB02785), anti-ATP6V0A1 (Santa Cruz Biotechnology, sc-374475), anti-His (MBL, M089), anti-Xpress (Invitrogen, #46–0528), anti-ACTB (ABM, G043).

Immunofluorescence and confocal microscopy

GFP-LC3B cells were grown on sterilized glass coverslips. After drug treatment, cells were fixed with 4% paraformaldehyde. For immunostaining, cells were blocked with 10% goat serum (Gibco, 16210) in phosphate-buffered saline (PBS; Wellgene, ML008), stained with a 1:500 dilution of primary antibody in PBS, and stained with a 1:1000 dilution of fluorescence-conjugated secondary antibody (Invitrogen, A11001, A11008, A11011, A11004, A11045, A11046). Finally, slides were washed 3 times with PBS, stained with DAPI and mounted in mounting medium (Vector, H-1000). Images were captured with a Carl Zeiss LSM710 confocal microscope (Oberkochem, Germany). The EEA1 antibody was purchased from BD (610457), and the LAMP1 antibody from Santa Cruz Biotechnology (sc-20011). To measure the extent of protein colocalization, confocal images were quantified using the Pearson correlation coefficient (PCC) as described previously.[32,33] PCC (R_r) values were calculated by WCIF ImageJ software (NIH, Bethesda, MD). The correlation coefficient was calculated from 5 cells per group.

RNA interference of *CREB* and semiquantitative RT-PCR

Small interfering RNAs (siRNAs) were purchased from ST PHARM (Seoul, Korea) and Bioneer (Daejeon, Korea). The nucleotide sequence for *CREB* siRNA #1 was 5'- CCA ACU CCA AUU UAC CAA A -3' and for *CREB* siRNA #2 was 5'-GCC UGC AAA CAU UAA CCA U -3'. The nucleotide sequence for *ITM2A* siRNA was 5'- CAU CUU UGC AGU UCU GUU A -3'. siRNA was transfected into HEK293 and HeLa cells using Lipofectamine RNAiMAX reagent (Invitrogen, 13778) in accordance with the manufacturer's instructions. For semiquantitative RT-PCR, cells were harvested and RNA was extracted using Trizol (Invitrogen, 15596) in accordance with the manufacturer's instructions, and subjected to reverse transcription-PCR (RT-PCR). *ITM2A* mRNA was amplified using the 5' primer CTT TGA AAA GGG AAT GAC TGC TTA C and the 3' primer TAC TAA CAT CAC GAA TTT CCT CCA C. Input RNA was normalized by amplifying ribosomal protein L4 (*RPL4*) RNA using the 5' primer GCT CTG GCC AGG GTG CTT TTG and the 3' primer ATG GCG TAT CGT TTT TGG GTT GT.

ChIP assay

Chromatin immunoprecipitation (ChIP) was performed using the ChIP Chromatin Immunoprecipitation kit (Millipore, 17–295) according to the manufacturer's standard protocol. HEK293 cells were either mock-treated or treated with forskolin (5 μM) for 4 h, and the nucleotide fragments (P1), including the CRE site in the *ITM2A* promoter, were amplified using the 5' primer ACT CCA CTT CCC CTG CTC TTC and the 3' primer TGT TAG CCC AAA CAG CAC TTA C. The control nucleotide fragments (P2) were amplified using the 5' primer TTA TGC CAA TCA CAG CAC AAG and the 3' primer TTG AAT GCC AAG CAA TGA TG.

Measurement of lysosomal pH

Quantification of lysosomal pH was performed with LysoSensor Yellow/Blue dextran (Life Technology, L-22460), according to previous protocols.[34] Briefly, 48 h after transfection, HEK293 cells were trypsinized and resuspended at 1×10^6/ml and incubated with 1 mg/ml of LysoSensor dextran for 1 h under growth conditions (37°C, 5% CO_2). To obtain the pH calibration curve, the cells were treated and equilibrated with 10 μM monesin and 10 μM nigerisin in MES buffer (5 mM NaCl, 115 mM KCl, 1.3 mM $MgSO_4$, and 25 mM MES), which was adjusted with pH from 3.5 to 6.5.[34,35] The samples were measured using Flex Station II (Molecular Devices, Sunnyvale, CA) with excitation at 335 nm and then the florescence emission intensity ratio of 450 nm/520 nm was calculated. The pH value of each sample was determined from the linear standard curve.

Statistical methods

The results of the luciferase assay, western blot and GFP-LC3B puncta analysis were evaluated by a 2-tailed t test using Microsoft Excel software. $P < 0.05$ was considered significant.

Disclosure of Potential conflicts of Interest

No potential conflicts of interest were disclosed.

Supplemental Material

Supplemental data for this article can be accessed on the publisher's website.

References

1. Klionsky DJ, Abdalla FC, Abeliovich H, Abraham RT, Acevedo-Arozena A, Adeli K, Agholme L, Agnello M, Agostinis P, Aguirre-Ghiso JA, et al. Guidelines for the use and interpretation of assays for monitoring autophagy. Autophagy 2012; 8:445-544; PMID:22966490; http://dx.doi.org/10.4161/auto.19496

2. Yamamoto A, Tagawa Y, Yoshimori T, Moriyama Y, Masaki R, Tashiro Y. Bafilomycin A1 prevents maturation of autophagic vacuoles by inhibiting fusion between autophagosomes and lysosomes in rat hepatoma cell line, H-4-II-E cells. Cell Struct Funct 1998; 23:33-42; PMID:9639028; http://dx.doi.org/10.1247/csf.23.33

3. Mizushima N, Yoshimori T, Levine B. Methods in mammalian autophagy research. Cell 2010; 140:313-26; PMID:20144757; http://dx.doi.org/10.1016/j.cell.2010.01.028

4. Kudo N, Barr AJ, Barr RL, Desai S, Lopaschuk GD. High rates of fatty acid oxidation during reperfusion of ischemic hearts are associated with a decrease in malonyl-CoA levels due to an increase in 5'-AMP-activated protein kinase inhibition of acetyl-CoA carboxylase. J Biol Chem 1995; 270:17513-20; PMID:7615556; http://dx.doi.org/10.1074/jbc.270.29.17513

5. Corton JM, Gillespie JG, Hardie DG. Role of the AMP-activated protein kinase in the cellular stress response. Curr Biol 1994; 4:315-24; PMID:7922340; http://dx.doi.org/10.1016/S0960-9822(00)00070-1

6. Kim J, Kundu M, Viollet B, Guan KL. AMPK and mTOR regulate autophagy through direct phosphorylation of Ulk1. Nat Cell Biol 2011; 13:132-41; PMID:21258367; http://dx.doi.org/10.1038/ncb2152

7. Jung CH, Ro SH, Cao J, Otto NM, Kim DH. mTOR regulation of autophagy. FEBS Lett 2010; 584:1287-95; PMID:20083114; http://dx.doi.org/10.1016/j.febslet.2010.01.017

8. Shaywitz AJ, Greenberg ME. CREB: a stimulus-induced transcription factor activated by a diverse array of extracellular signals. Annu Rev Biochem 1999; 68:821-61; PMID:10872467; http://dx.doi.org/10.1146/annurev.biochem.68.1.821

9. Mayr B, Montminy M. Transcriptional regulation by the phosphorylation-dependent factor CREB. Nat Rev Mol Cell Biol 2001; 2:599-609; PMID:11483993; http://dx.doi.org/10.1038/35085068

10. Stephan JS, Yeh YY, Ramachandran V, Deminoff SJ, Herman PK. The Tor and PKA signaling pathways independently target the Atg1/Atg13 protein kinase complex to control autophagy. Proc Natl Acad Sci U S A 2009; 106:17049-54; PMID:19805182; http://dx.doi.org/10.1073/pnas.0903316106

11. Mizushima N. The role of the Atg1/ULK1 complex in autophagy regulation. Curr Opin Cell Biol 2010; 22:132-9; PMID:20056399; http://dx.doi.org/10.1016/j.ceb.2009.12.004

12. Budovskaya YV, Stephan JS, Deminoff SJ, Herman PK. An evolutionary proteomics approach identifies substrates of the cAMP-dependent protein kinase. Proc Natl Acad Sci U S A 2005; 102:13933-8; PMID:16172400; http://dx.doi.org/10.1073/pnas.0501046102

13. Shahnazari S, Namolovan A, Mogridge J, Kim PK, Brumell JH. Bacterial toxins can inhibit host cell autophagy through cAMP generation. Autophagy 2011; 7:957-65; PMID:21606683; http://dx.doi.org/10.4161/auto.7.9.16435

14. Shelburne JD, Arstila AU, Trump BF. Studies on cellular autophagocytosis. Cyclic AMP- and dibutyryl cyclic AMP-stimulated autophagy in rat liver. Am J Pathol 1973; 72:521-40; PMID:4125701

15. Deleersnijder W, Hong GZ, Cortvrindt R, Poirier C, Tylzanowski P, Pittois K, Van Marck E, Merregaert J. Isolation of markers for chondro-osteogenic differentiation using cDNA library subtraction - Molecular cloning and characterization of a gene belonging to a novel multigene family of integral membrane proteins. J Biol Chem 1996; 271:19475-82; PMID:8702637; http://dx.doi.org/10.1074/jbc.271.32.19475

16. Lagha M, Mayeuf-Louchart A, Chang T, Montarras D, Rocancourt D, Zalc A, Kormish J, Zaret KS, Buckingham ME, Relaix F. Itm2a Is a Pax3 Target Gene, Expressed at Sites of Skeletal Muscle Formation In Vivo. PLoS One 2013; 8:e63143; PMID:23650549; http://dx.doi.org/10.1371/journal.pone.0063143

17. Van den Plas D, Merregaert J. Constitutive overexpression of the integral membrane protein Itm2A enhances myogenic differentiation of C2C12 cells. Cell Biol Int 2004; 28:199-207; PMID:14984746; http://dx.doi.org/10.1016/j.cellbi.2003.11.019

18. Boeuf S, Borger M, Hennig T, Winter A, Kasten P, Richter W. Enhanced ITM2A expression inhibits chondrogenic differentiation of mesenchymal stem cells. Differentiation 2009; 78:108-15; PMID:19541402; http://dx.doi.org/10.1016/j.diff.2009.05.007

19. Kirchner J, Bevan MJ. ITM2A is induced during thymocyte selection and T cell activation and causes downregulation of CD8 when overexpressed in CD4(+) CD8(+) double positive thymocytes. J Exp Med 1999; 190:217-28; PMID:10432285; http://dx.doi.org/10.1084/jem.190.2.217

20. Tai TS, Pai SY, Ho IC. Itm2a, a Target Gene of GATA-3, Plays a Minimal Role in Regulating the Development and Function of T Cells. PLoS One 2014; 9:e96535; PMID:24831988; http://dx.doi.org/10.1371/journal.pone.0096535

21. Dreos R, Ambrosini G, Cavin Perier R, Bucher P. EPD and EPDnew, high-quality promoter resources in the next-generation sequencing era. Nucleic Acids Res 2013; 41:D157-64; PMID:23193273; http://dx.doi.org/10.1093/nar/gks1233

22. Zambon AC, Zhang L, Minovitsky S, Kanter JR, Prabhakar S, Salomonis N, Vranizan K, Dubchak I, Conklin BR, Insel PA. Gene expression patterns define key transcriptional events in cell-cycle regulation by cAMP and protein kinase A. Proc Natl Acad Sci U S A 2005; 102:8561-6; PMID:15939874; http://dx.doi.org/10.1073/pnas.0503363102

23. Kimura S, Noda T, Yoshimori T. Dissection of the autophagosome maturation process by a novel reporter protein, tandem fluorescent-tagged LC3. Autophagy 2007; 3:452-60; PMID:17534139; http://dx.doi.org/10.4161/auto.4451

24. Franceschini A, Szklarczyk D, Frankild S, Kuhn M, Simonovic M, Roth A, Lin J, Minguez P, Bork P, von Mering C, et al. STRING v9.1: protein-protein interaction networks, with increased coverage and integration. Nucleic Acids Res 2013; 41:D808-15; PMID:23203871; http://dx.doi.org/10.1093/nar/gks1094

25. Ochotny N, Voronov I, Owen C, Aubin JE, Manolson MF. The R740S mutation in the V-ATPase a3 subunit results in osteoclast apoptosis and defective early-stage autophagy. J Cell Biochem 2013; 114:2823-33; PMID:23908015; http://dx.doi.org/10.1002/jcb.24630

26. Liang C, Lee JS, Inn KS, Gack MU, Li Q, Roberts EA, Vergne I, Deretic V, Feng P, Akazawa C, et al. Beclin1-binding UVRAG targets the class C Vps complex to coordinate autophagosome maturation and endocytic trafficking. Nat Cell Biol 2008; 10:776-87; PMID:18552835; http://dx.doi.org/10.1038/ncb1740

27. Klionsky DJ, Elazar Z, Seglen PO, Rubinsztein DC. Does bafilomycin A1 block the fusion of autophagosomes with lysosomes? Autophagy 2008; 4:849-50; PMID:18758232; http://dx.doi.org/10.4161/auto.6845

28. Mizushima N, Levine B. Autophagy in mammalian development and differentiation. Nat Cell Biol 2010; 12:823-30; PMID:20811354; http://dx.doi.org/10.1038/ncb0910-823

29. Masiero E, Agatea L, Mammucari C, Blaauw B, Loro E, Komatsu M, Metzger D, Reggiani C, Schiaffino S, Sandri M. Autophagy Is Required to Maintain Muscle Mass. Cell Metabolism 2009; 10:507-15; PMID:19945408; http://dx.doi.org/10.1016/j.cmet.2009.10.008

30. Yoon JH, Her S, Kim M, Jang IS, Park J. The expression of damage-regulated autophagy modulator 2 (DRAM2) contributes to autophagy induction. Mol Biol Rep 2011; 39:1087-93; PMID:21584698; http://dx.doi.org/10.1007/s11033-011-0835-x

31. Kabeya Y, Mizushima N, Ueno T, Yamamoto A, Kirisako T, Noda T, Kominami E, Ohsumi Y, Yoshimori T. LC3, a mammalian homologue of yeast Apg8p, is localized in autophagosome membranes after processing. EMBO J 2000; 19:5720-8; PMID:11060023; http://dx.doi.org/10.1093/emboj/19.21.5720

32. Dunn KW, Kamocka MM, McDonald JH. A practical guide to evaluating colocalization in biological microscopy. Am J Physiol Cell Physiol 2011; 300:C723-42; PMID:21209361; http://dx.doi.org/10.1152/ajpcell.00462.2010

33. Kanda VA, Lewis A, Xu X, Abbott GW. KCNE1 and KCNE2 inhibit forward trafficking of homomeric N-type voltage-gated potassium channels. Biophys J 2011; 101:1354-63; PMID:21943416; http://dx.doi.org/10.1016/j.bpj.2011.08.015

34. Lee JH, Yu WH, Kumar A, Lee S, Mohan PS, Peterhoff CM, Wolfe DM, Martinez-Vicente M, Massey AC, Sovak G, et al. Lysosomal proteolysis and autophagy require presenilin 1 and are disrupted by Alzheimer-related PS1 mutations. Cell 2010; 141:1146-58; PMID:20541250; http://dx.doi.org/10.1016/j.cell.2010.05.008

35. Diwu Z, Chen CS, Zhang C, Klaubert DH, Haugland RP. A novel acidotropic pH indicator and its potential application in labeling acidic organelles of live cells. Chem Biol 1999; 6:411-8; PMID:10381401; http://dx.doi.org/10.1016/S1074-5521(99)80059-3